Supporting Information

Temperature Independent Catalytic Two-Electron Reduction of Dioxygen by Ferrocenes with a Tris[2-(2-pyridyl)ethyl]amine-Copper(II) Catalyst in the Presence of Perchloric Acid

Dipanwita Das,[†] Yong-Min Lee,[†] Kei Ohkubo,[§] Wonwoo Nam,*[,†] and Kenneth D. Karlin,*[,†,‡] and Shunichi Fukuzumi*[,†,§]

[†]*Department of Bioinspired Science, Ewha Womans University, Seoul 120-750, Korea*

[‡]*Department of Chemistry, The Johns Hopkins University, Baltimore, MD 21218, USA*

[§]*Department of Material and Life Science, Division of Advanced Science and Biotechnology, Graduate School of Engineering, Osaka University, Suita, Osaka 565-0871, Japan*

*E-mail addresses: fukuzumi@chem.eng.osaka-u.ac.jp; karlin@jhu.edu; wwnam@ewha.ac.kr

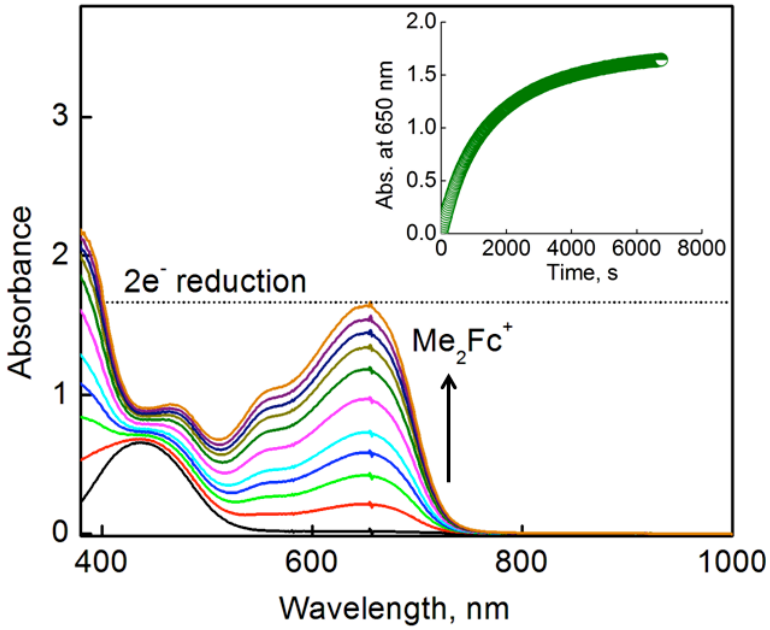

Figure S1. Absorption spectral changes in the two-electron reduction of O_2 ($[O_2]$ = 2.2 mM) by Me_2Fc (10 mM) with **1** (0.040 mM) in the presence of $HClO_4$ (40 mM) in acetone at 298 K. The inset shows the time profile of absorbance at 650 nm due to Me_2Fc^+.

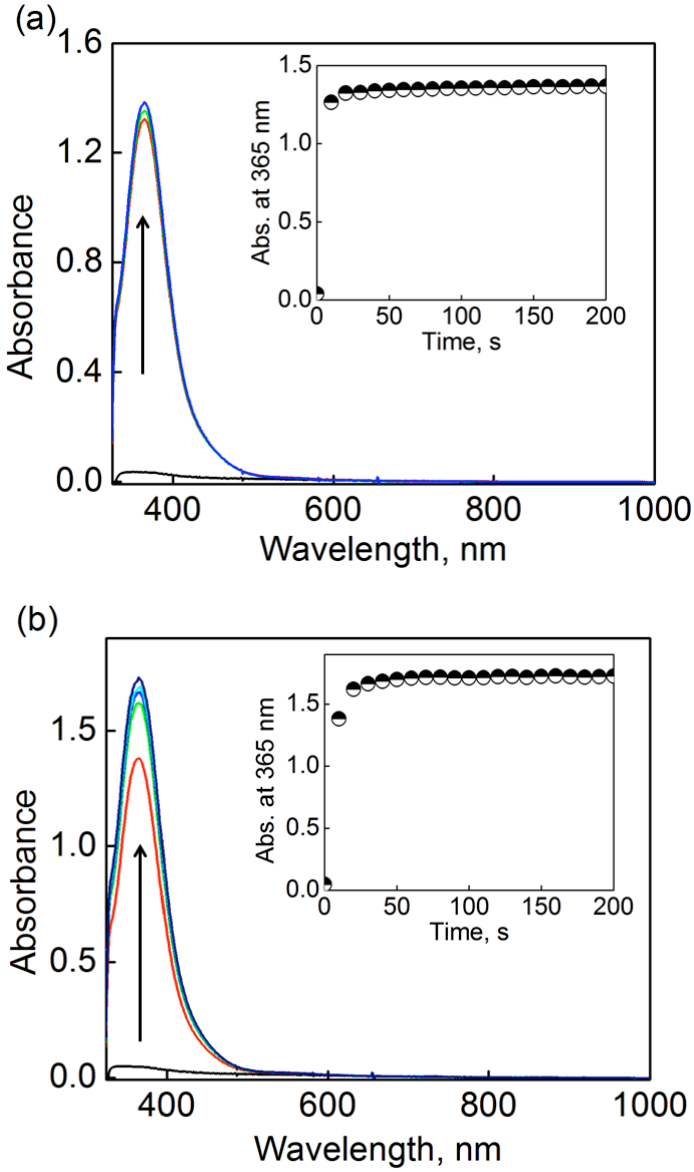

Figure S2. (a) Spectral changes observed in the reaction of NaI (0.20 M) with the diluted (40 times) acetone solution of the products at 298 K after the catalytic reduction of O_2 (2.2 mM) by Me_2Fc (10 mM) with **1** (0.040 mM) in the presence of excess $HClO_4$ (40 mM) in acetone at 298 K. (b) Spectral changes observed in the reaction of the NaI (0.20 M) with H_2O_2 (0.068 mM) in acetone at 298 K.

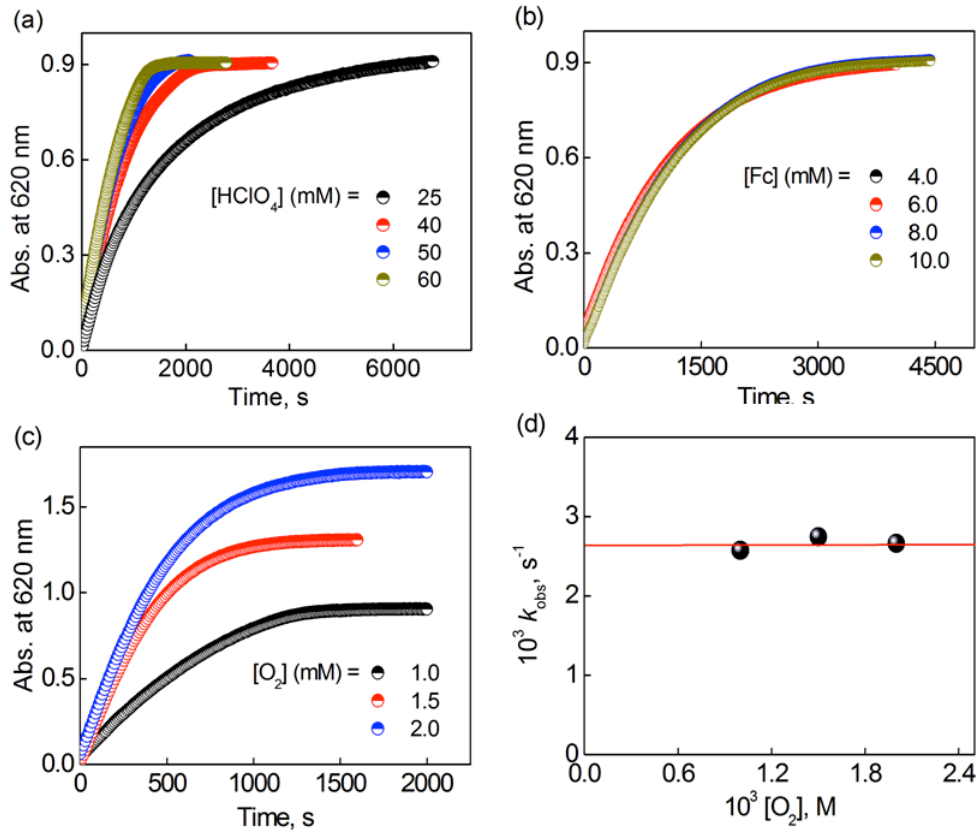

Figure S3. (a) Time profiles of the absorbance at 620 nm due to Fc^+ in the two-electron reduction of O_2 catalyzed by **1** (0.10 mM) with Fc (10 mM) in the presence of various concentrations of $HClO_4$ (25 mM (black), 40 mM (red), 50 mM (blue) and 60 mM (dark yellow)) in an acetone solution containing O_2 ($[O_2]$ = 1.0 mM) at 298 K. (b) Time profiles of the absorbance at 620 nm due to Fc^+ in the two-electron reduction of O_2 ($[O_2]$ = 1.0 mM) catalyzed by **1** (0.10 mM) with Fc (4.0 mM (black), 6.0 mM (red), 8.0 mM (blue) and 10 mM (dark yellow)) in the presence of $HClO_4$ (40 mM) in an acetone solution at 298 K. (c) Time profiles of the absorbance at 620 nm due to Fc^+ in the two-electron reduction of O_2 (1.0 mM (black), 1.5 mM (red) and 2.0 mM (blue)) catalyzed by **1** (0.10 mM) with Fc (10 mM) in the presence of $HClO_4$ (60 mM) in an acetone solution at 298 K and (d) plot of k_{obs} versus $[O_2]$ for the two-electron reduction of O_2 catalyzed by **1** (0.10 mM) with Fc (10 mM) in the presence of $HClO_4$ (60 mM) in an acetone solution at 298 K.

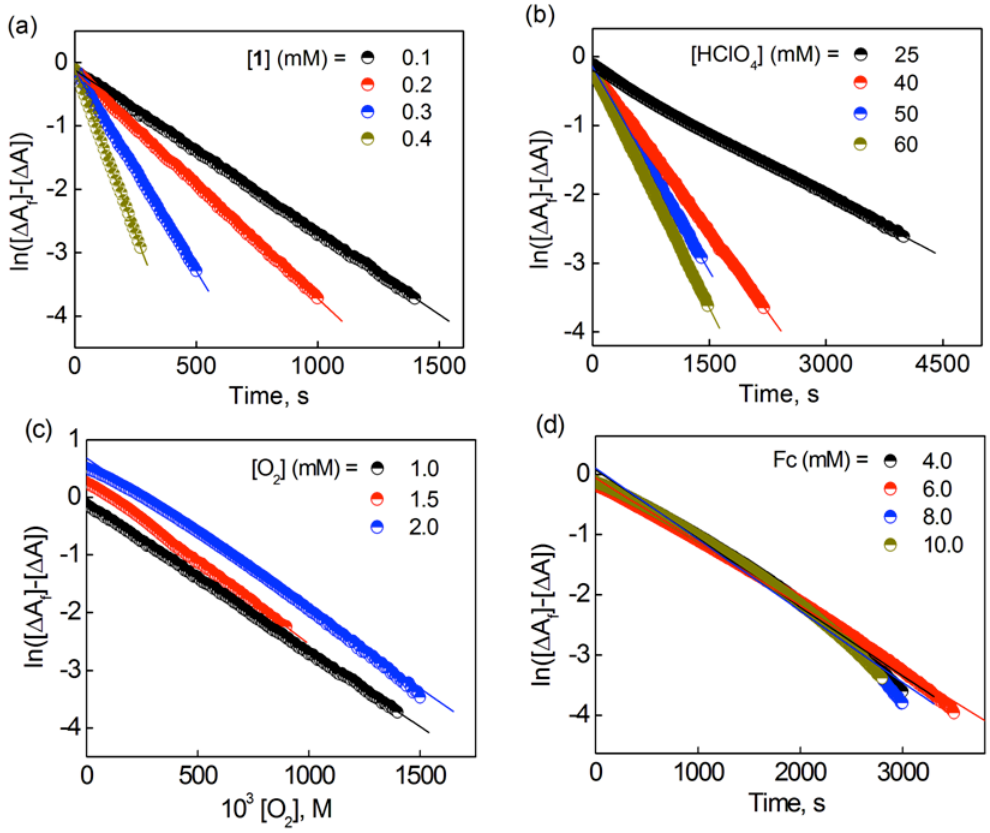

Figure S4. First-order plots of the formation of Fc^+ at 298 K in the two-electron reduction of O_2 catalyzed by (a) **1** (0.10 mM (black), 0.20 mM (red), 0.30 mM (blue) and 0.40 mM (dark yellow)) with Fc (10 mM) in the presence of $HClO_4$ (60 mM) in an acetone solution containing O_2 ($[O_2]$ = 1.0 mM), (b) **1** (0.10 mM) with Fc (10 mM) in the presence of various concentrations of $HClO_4$ (25 mM (black), 40 mM (red), 50 mM (blue) and 60 mM (dark yellow)) in an acetone solution containing O_2 ($[O_2]$ = 1.0 mM), (c) **1** (0.10 mM) with Fc (10 mM) in the presence of $HClO_4$ (60 mM) in an acetone solution having various concentrations of O_2 (1.0 mM (black), 1.5 mM (red) and 2.0 mM (blue)) and (d) **1** (0.10 mM) with Fc (4.0 mM (black), 6.0 mM (red), 8.0 mM (blue) and 10 mM (dark yellow)) in the presence of $HClO_4$ (40 mM) in an acetone solution.

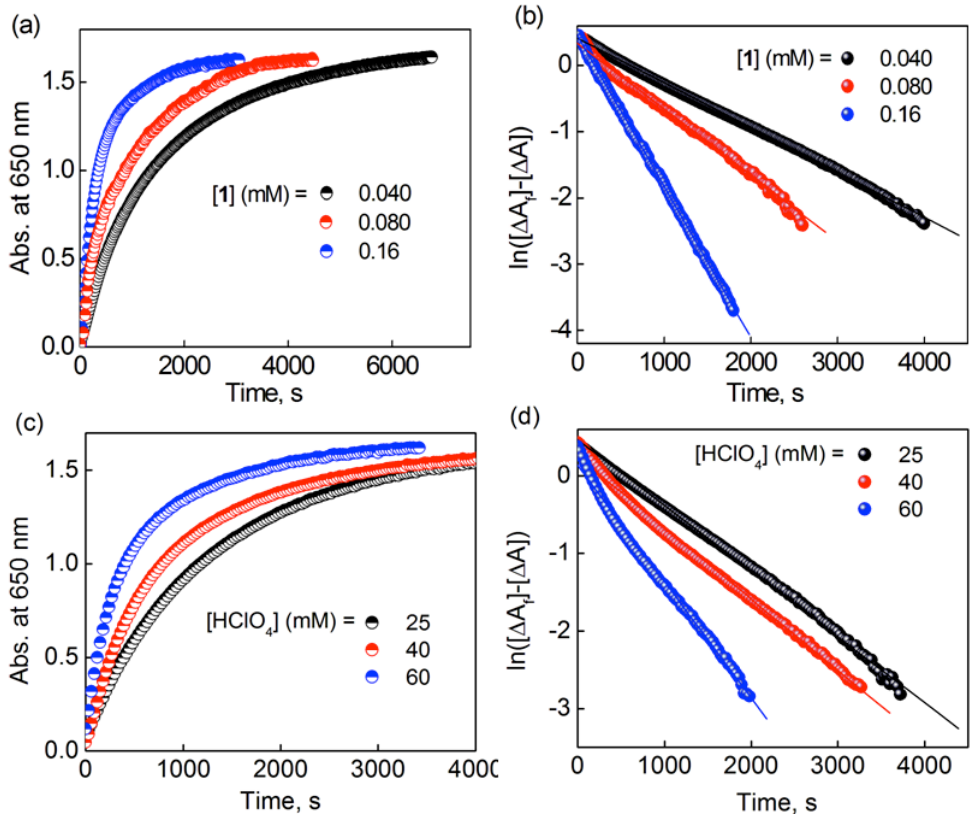

Figure S5. (a) Time profiles of the absorbance at 650 nm due to Me_2Fc^+ and (b) first-order plots of the formation of Me_2Fc^+ in the two-electron reduction of O_2 catalyzed by **1** (0.040 mM (black), 0.080 mM (red) and 0.16 mM (blue)), with Me_2Fc (10 mM) in the presence of $HClO_4$ (40 mM) in an acetone solution ($[O_2]$ = 2.2 mM) at 298 K. (c) Time profiles of the absorbance at 650 nm due to Me_2Fc^+ and (d) first-order plots of the formation of Me_2Fc^+ in the two-electron reduction of O_2 catalyzed by **1** (0.080 mM) with Me_2Fc (10 mM) in the presence of various concentrations of $HClO_4$ (25 mM (black), 40 mM (red) and 60 mM (blue)) in an acetone solution containing O_2 ($[O_2]$ = 2.2 mM) at 298 K.

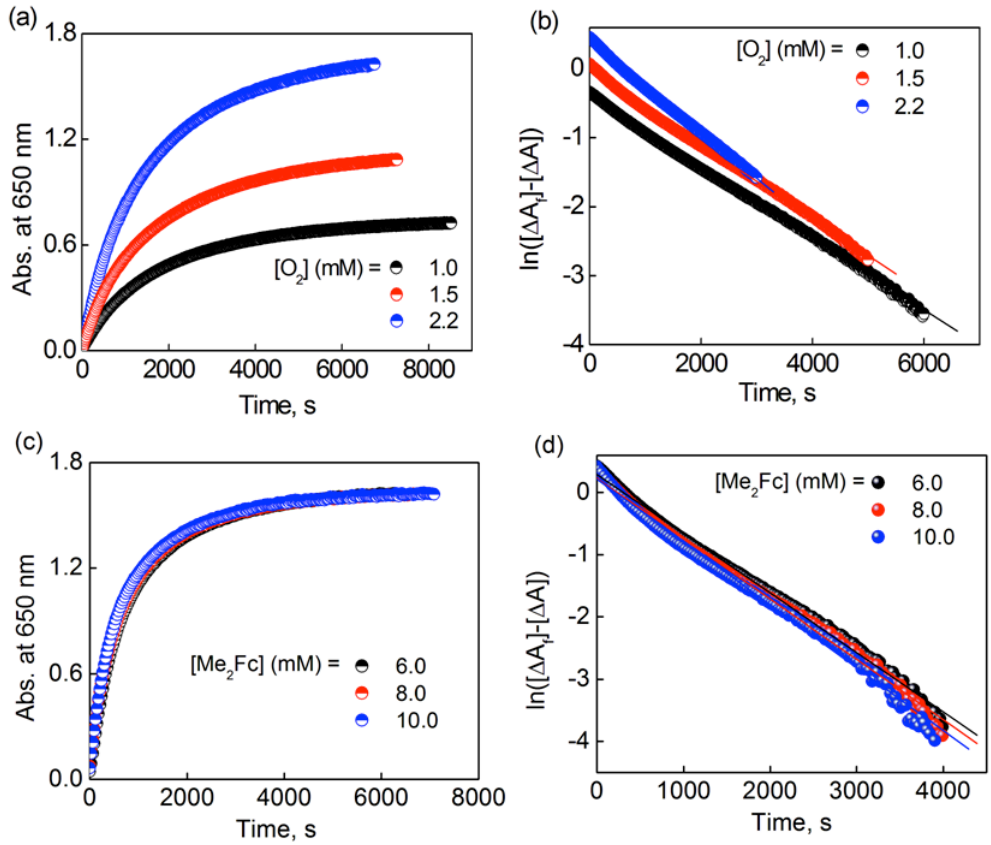

Figure S6. (a) Time profiles of the absorbance at 650 nm due to Me_2Fc^+ and (b) first-order plots of the formation of Me_2Fc^+ in the two-electron reduction of O_2 (1.0 mM (black), 1.5 mM (red) and 2.2 mM (blue)) catalyzed by **1** (0.040 mM) with Me_2Fc (10 mM) in the presence of $HClO_4$ (40 mM) in an acetone solution at 298 K. (c) Time profiles of the absorbance at 650 nm due to Me_2Fc^+ and (b) first-order plots of the formation of Me_2Fc^+ in the two-electron reduction of O_2 ($[O_2]$ = 2.2 mM) catalyzed by **1** (0.040 mM) with Me_2Fc (6.0 mM (black), 8.0 mM (red) and 10 mM (blue)) in the presence of $HClO_4$ (40 mM) in an acetone solution at 298 K.

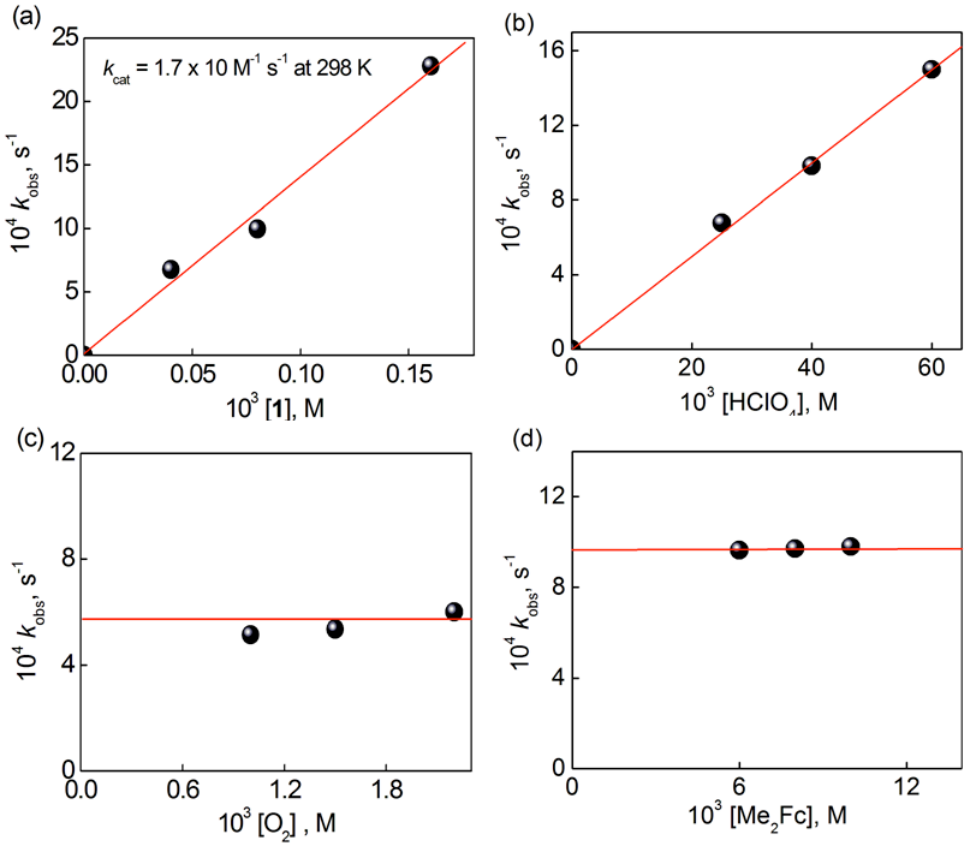

Figure S7. (a) Plot of k_{obs} versus [**1**] for the two-electron reduction of O_2 ([O_2] = 2.2 mM) catalyzed by **1** with Me_2Fc (10 mM) in the presence of $HClO_4$ (40 mM) in an acetone solution at 298 K. (b) Plot of k_{obs} versus [$HClO_4$] for the two-electron reduction of O_2 by Me_2Fc (10 mM) catalyzed by **1** (0.080 mM) in an acetone solution containing O_2 (2.2 mM) at 298 K. (c) Plot of k_{obs} versus [O_2] for the two-electron reduction of O_2 catalyzed by **1** (0.040 mM) with Me_2Fc (10 mM) in the presence of $HClO_4$ (40 mM) in an acetone solution at 298 K. (d) Plot of k_{obs} versus [Me_2Fc] for the two-electron reduction of O_2 catalyzed by **1** (0.040 mM) with Me_2Fc in the presence of $HClO_4$ (40 mM) in an acetone solution containing O_2 ([O_2] = 2.2 mM) at 298 K.

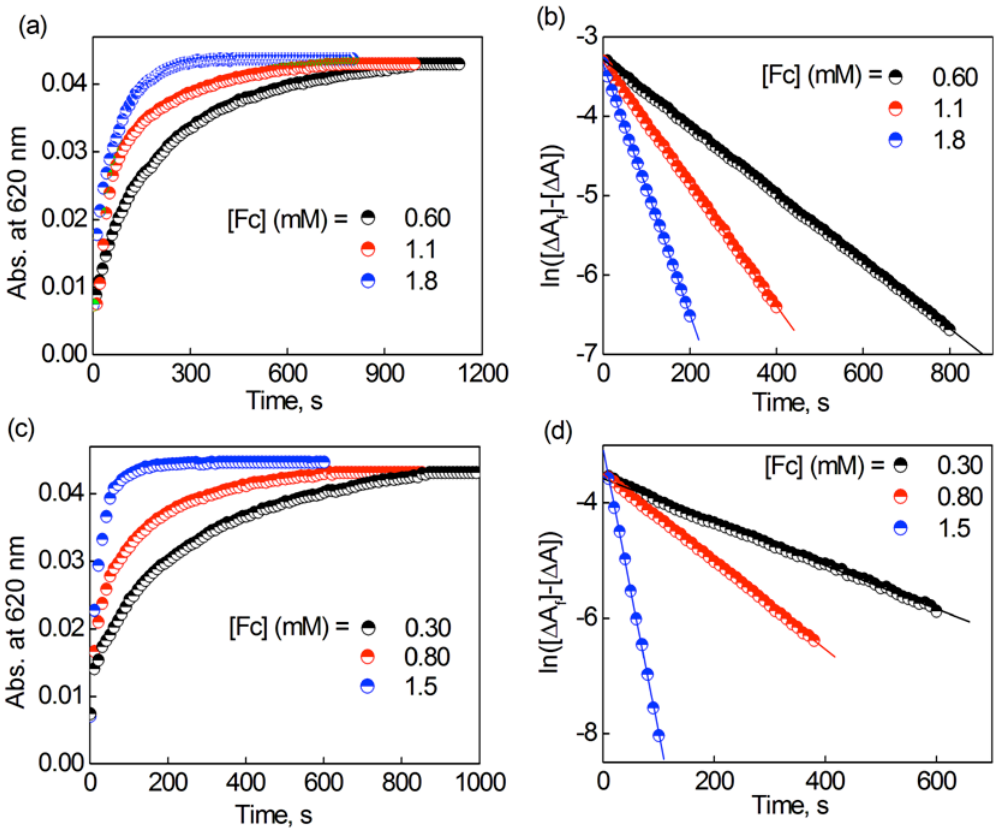

Figure S8. (a) Time profiles of the absorbance at 620 nm due to Fc^+ and (b) first-order plots of the formation of Fc^+ in the electron transfer reaction from Fc (0.60 mM (black), 1.1 mM (red) and 1.8 mM (blue)) to **1** (0.10 mM) in acetone at 193 K. (c) Time profiles of the absorbance at 620 nm due to Fc^+ and (d) first-order plots of the formation of Fc^+ in the electron transfer reaction from Fc (0.30 mM (black), 0.80 mM (red) and 1.5 mM (blue)) to **1** (0.10 mM) in acetone at 203 K.

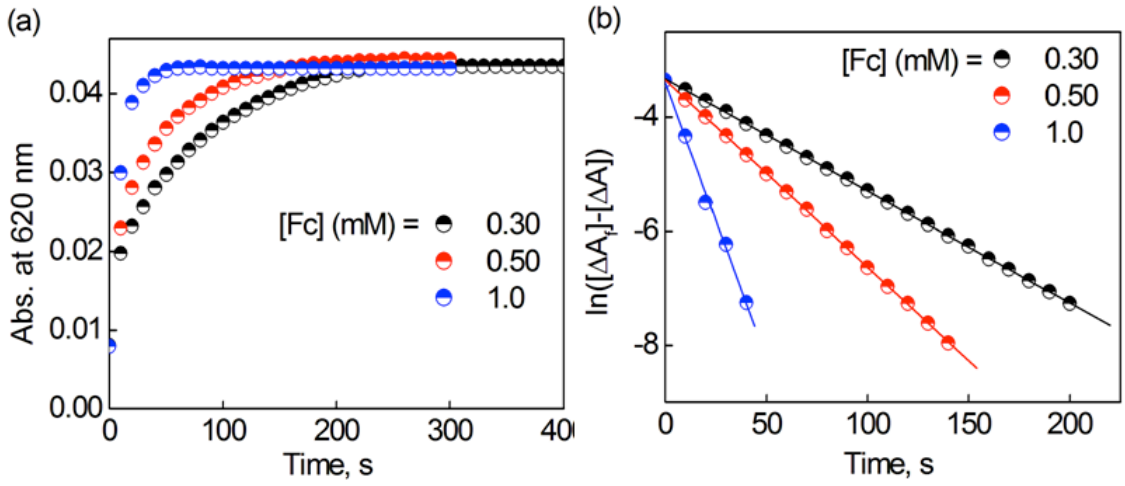

Figure S9. (a) Time profiles of the absorbance at 620 nm due to Fc^+ and (b) first-order plots of the formation of Fc^+ in the electron transfer reaction from Fc (0.30 mM (black), 0.50 mM (red) and 1.0 mM (blue)) to **1** (0.10 mM) in acetone at 213 K.

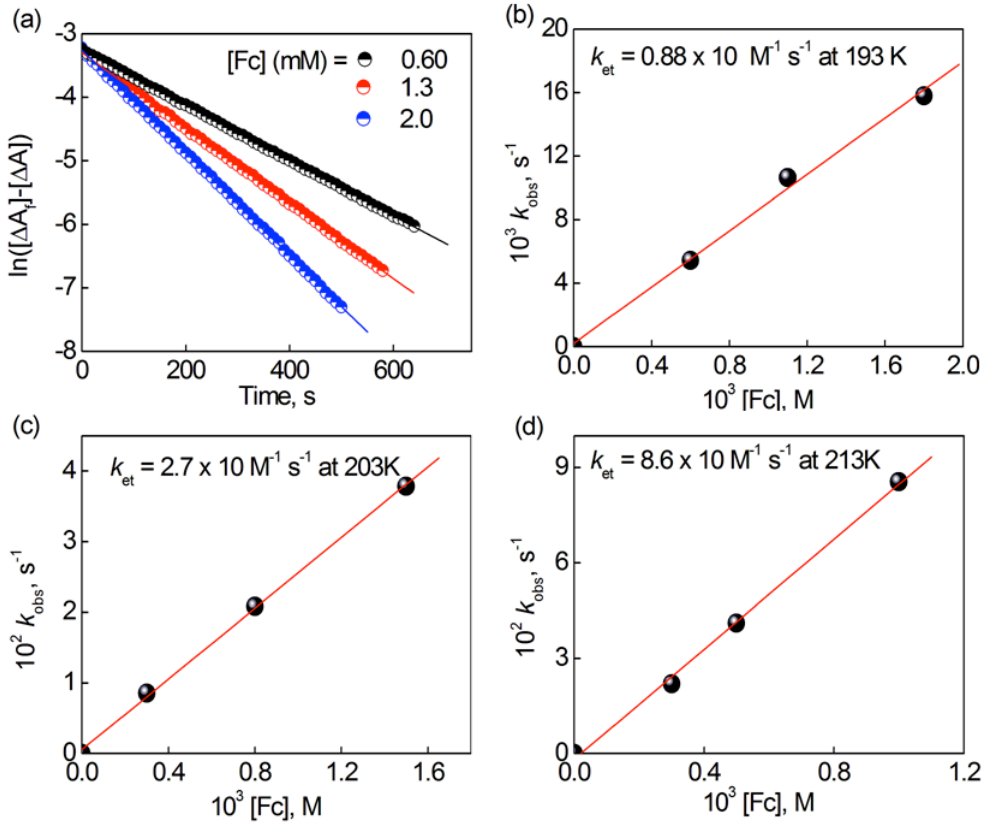

Figure S10. (a) First-order plots of the formation of Fc^+ in the electron transfer reaction from Fc (0.60 mM (black), 1.3 mM (red) and 2.0 mM (blue)) to **1** (0.10 mM) in acetone at 183 K. (b,c,d) Plot of k_{obs} versus [Fc] in the electron transfer from Fc to $[Cu^{II}(tepa)]^{2+}$ (**1**) (0.10 mM) in an acetone solution at (b) 193 K, (c) 203 K and (d) 213 K.

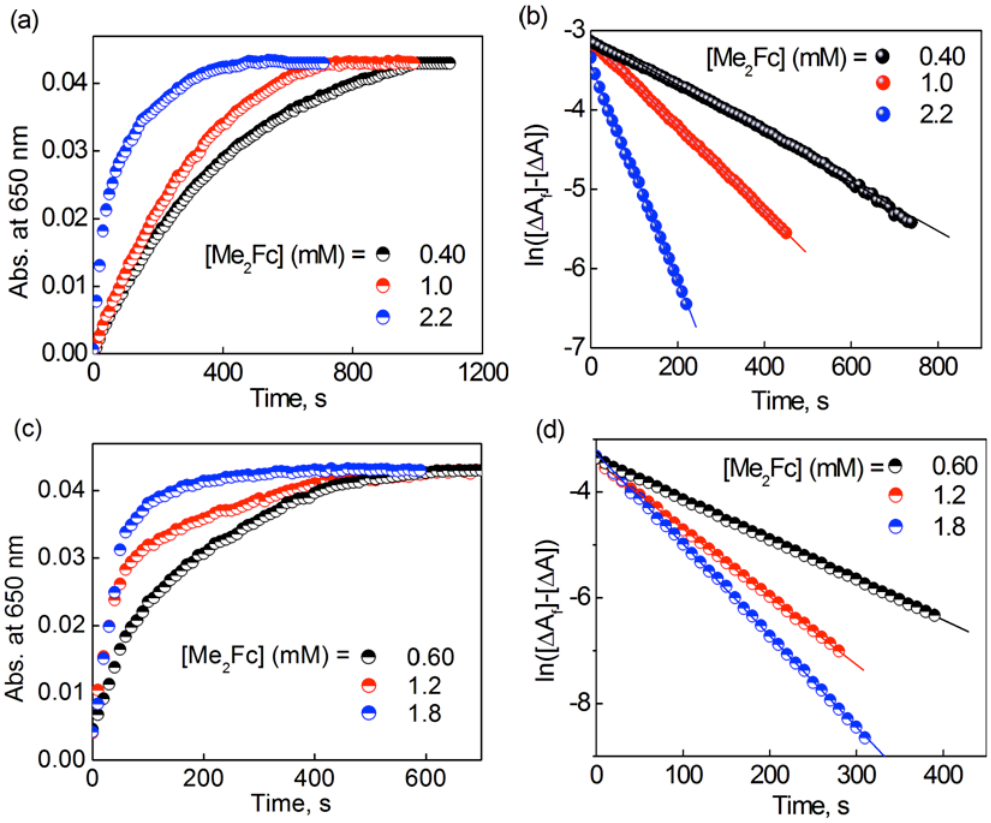

Figure S11. (a) Time profiles of the absorbance at 650 nm due to Me_2Fc^+ and (b) first-order plots of the formation of Me_2Fc^+ in the electron transfer reaction from Me_2Fc (0.40 mM (black), 1.0 mM (red) and 2.2 mM (blue)) to **1** (0.12 mM) in acetone at 183 K. (c) Time profiles of the absorbance at 650 nm due to Me_2Fc^+ and (d) first-order plots of the formation of Me_2Fc^+ in the electron transfer reaction from Me_2Fc (0.60 mM (black), 1.2 mM (red) and 1.8 mM (blue)) to **1** (0.12 mM) in acetone at 193 K.

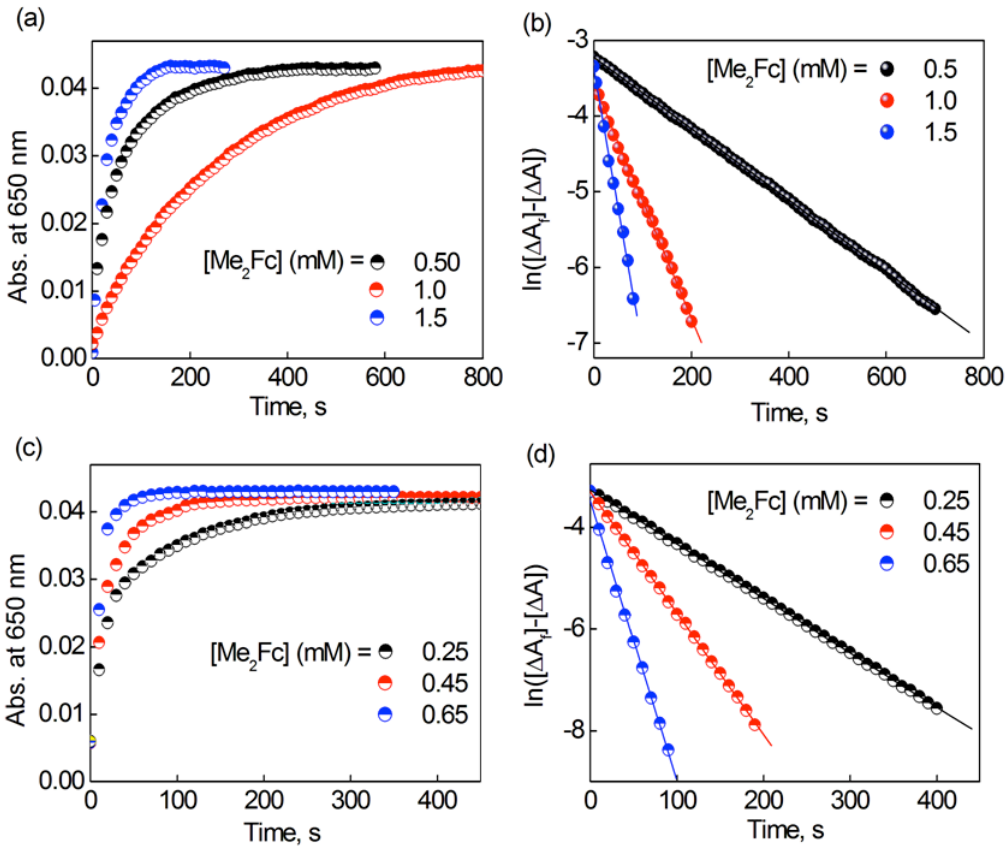

Figure S12. (a) Time profiles of the absorbance at 650 nm due to Me_2Fc^+ and (b) first-order plots of the formation of Me_2Fc^+ in the electron transfer reaction from Me_2Fc (0.50 mM (black), 1.0 mM (red) and 1.5 mM (blue)) to **1** (0.12 mM) in acetone at 203 K. (c) Time profiles of the absorbance at 650 nm due to Me_2Fc^+ and (d) first-order plots of the formation of Me_2Fc^+ in the electron transfer reaction from Me_2Fc (0.25 mM (black), 0.45 mM (red) and 0.65 mM (blue)) to **1** (0.12 mM) in acetone at 213 K.

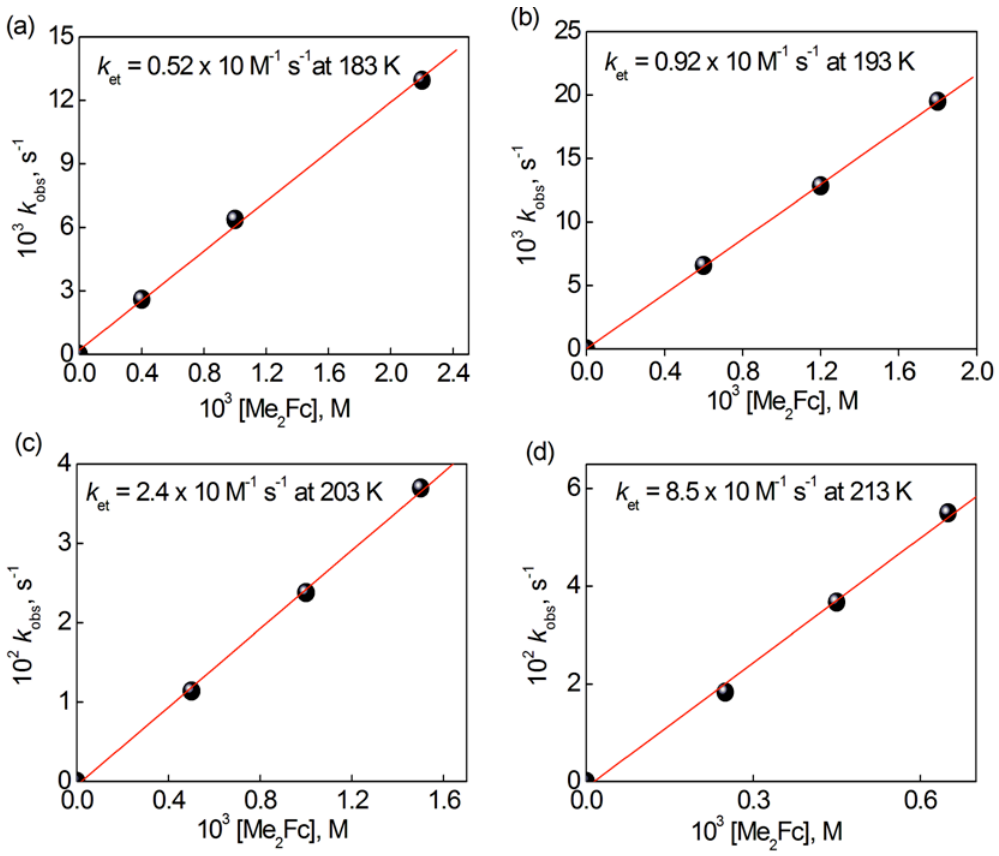

Figure S13. Plot of k_{obs} versus [Me_2Fc] in the electron transfer from Me_2Fc to $[Cu^{II}(tepa)]^{2+}$ (**1**) (0.12 mM) in an acetone solution at (a)183 K, (b) 193 K, (c) 203 K and (d) 213 K.

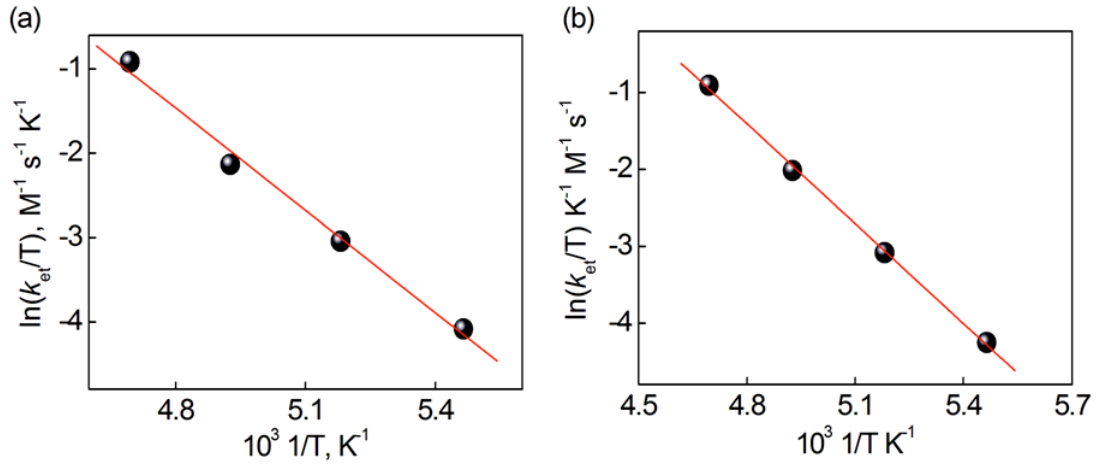

Figure S14. Eyring plot, ln(k_{et}/T) vs 1/T, of the rate constants (k_{et}) of electron transfer from (a) Me_2Fc and (b) Fc to **1** in acetone.

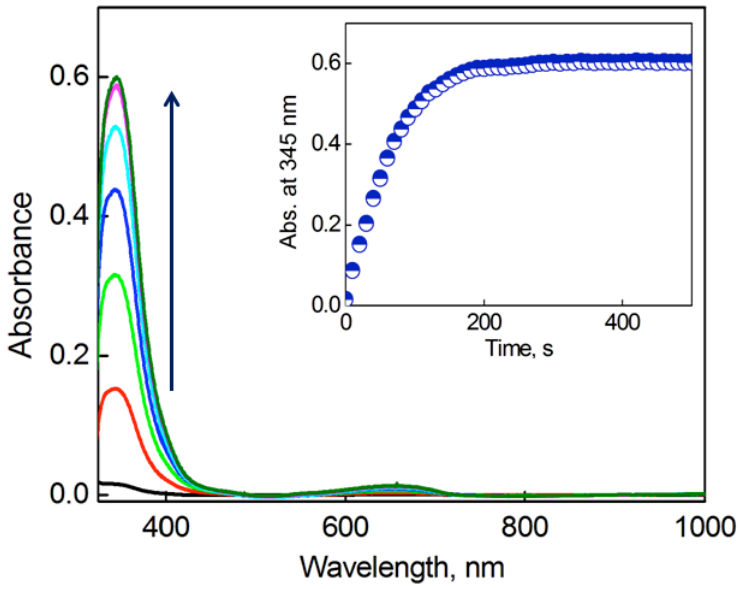

Figure S15. Formation of the hydroperoxo complex, $[Cu^{II}(tepa)(OOH)]^{+}$ (**3**) (λ_{max}=345 nm) in the reaction of $[Cu^{I}(tepa)]^{+}$ (0.16 mM), which was generated by reacting $[Cu^{II}(tepa)]^{2+}$ (0.16 mM) with Fc (0.16 mM) at 298K, with O_2 (2.2 mM) in presence of $HClO_4$ (3.0 mM) in acetone at 193 K. Inset shows the time profile of the absorbance at 345 nm due to **3**.

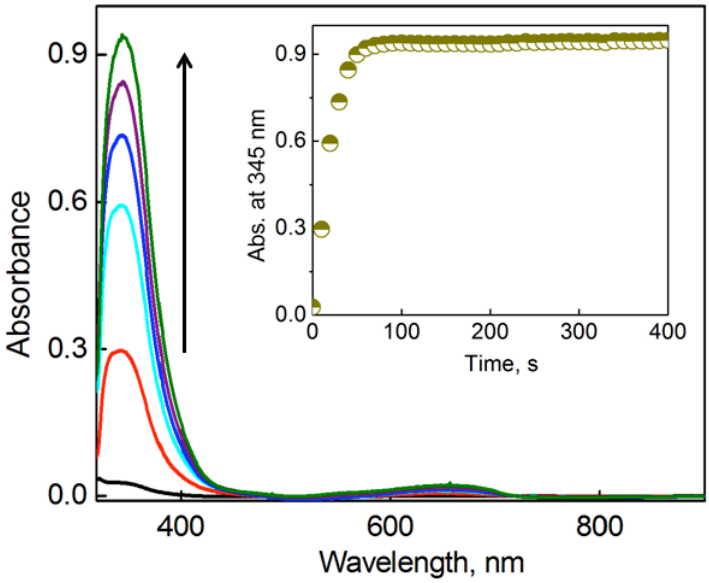

Figure S16. Spectral change observed in the reaction of $[Cu^{II}(tepa)]^{2+}$ (**1**) (0.13 mM) with H_2O_2 (1.3 mM) in the presence of Me_4NOH (0.26 mM) in acetone at 193 K. Inset shows the time profile for the formation of $[Cu^{II}(tepa)(OOH)]^{+}$ (**3**) at 345 nm.

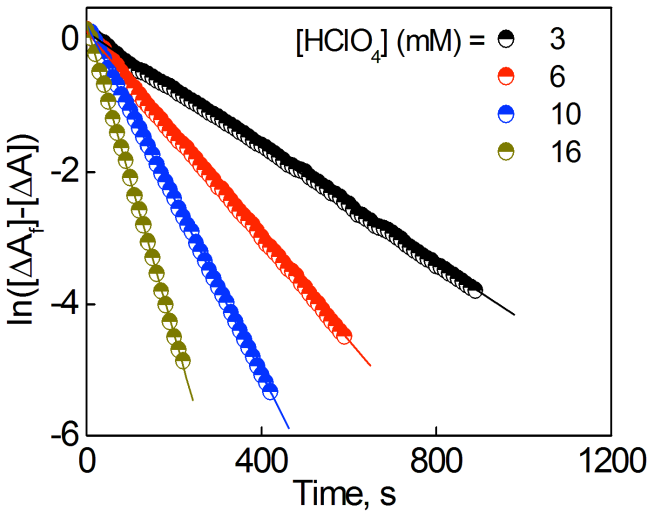

Figure S17. First-order plots of the formation of $[Cu^{II}(tepa)(OOH)]^{+}$ (**3**) for the O_2 (2.2 mM) binding step to $[Cu^{I}(tepa)]^{+}$ (**2**) (0.18 mM) ($[Cu^{I}(tepa)]^{+}$ was generated by room temperature mixing of $[Cu^{II}(tepa)]^{2+}$ (0.18 mM) with Fc (0.36 mM)) in the presence of various concentrations of $HClO_4$ (3.0 mM (black), 6.0 mM (red), 10 mM (blue) and 16 mM (dark yellow)) in an acetone solution at 193 K.

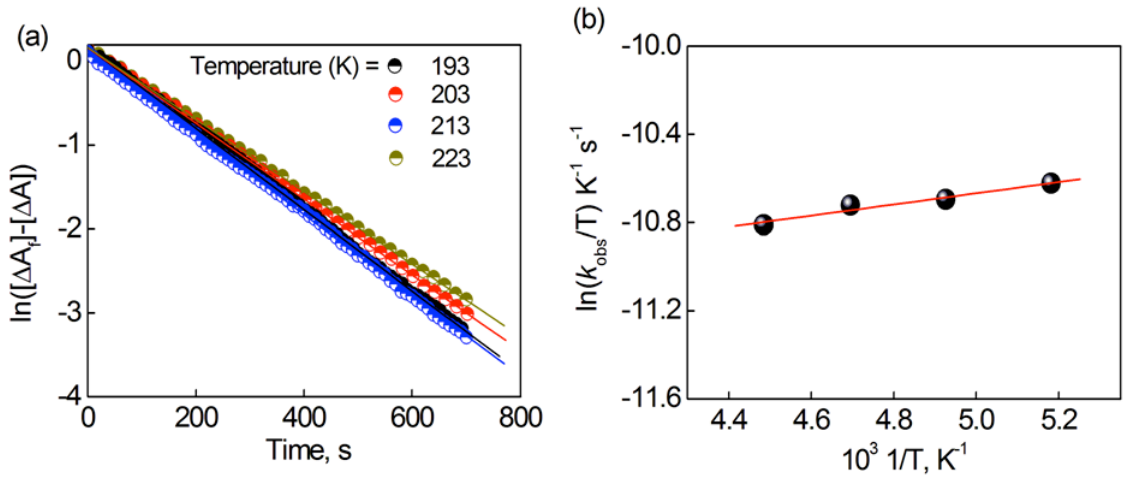

Figure S18. (a) First-order plots of the formation of $[Cu^{II}(tepa)(OOH)]^+$ in the O_2 ($[O_2]$ = 2.2 mM) binding step in presence of $HClO_4$ (3.0 mM) with $[Cu^{I}(tepa)]^+$ (**2**) (0.16 mM) ($[Cu^{I}(tepa)]^+$ was produced from room temperature mixing of $[Cu^{II}(tepa)]^{2+}$ (0.16 mM) with Fc (0.32 mM)) at different temperatures (193 K (black), 203 K (red), 213 K (blue) and 223 K (dark yellow)). (b) Eyring plot, $\ln(k_{obs}/T)$ vs 1/T, of the rate constants (k_{obs}) obtained from O_2 binding to **2** with $HClO_4$ in acetone.

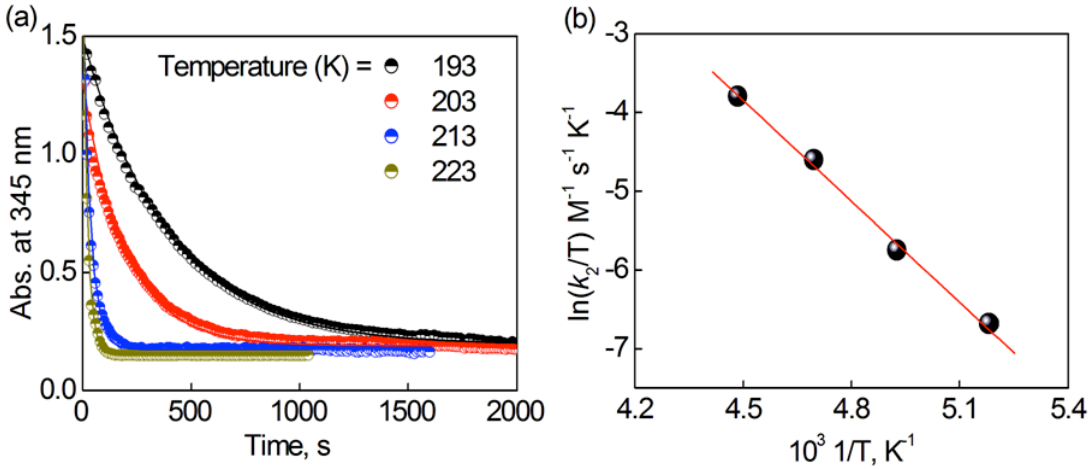

Figure S19. (a) Time profiles of the decay of $[Cu^{II}(tepa)(OOH)]^+$ (**3**; 0.20 mM) monitored at 345 nm in presence of $HClO_4$ (8.0 mM) at different temperatures (193 K (black), 203 K (red), 213 K (blue) and 223 K (dark yellow)). (b) Eyring plot, $\ln(k_2/T)$ vs 1/T, of the rate constants (k_2) obtained from protonation of **3** (0.20 mM) with $HClO_4$ (8.0 mM) in acetone.